

A Model for ‘Antagonistic’ Protein Dynamics

P. RASHKOV¹, B. A. SCHMITT², L. SØGAARD-ANDERSEN³, P. LENZ⁴, & S. DAHLKE⁵

ABSTRACT: The MglA and MglB proteins that regulate motility in the rod-shaped cells of *Myxococcus xanthus* localize to opposite cell poles. During the irregularly occurring cellular reversals, the two proteins switch poles. The concentration profiles of the two proteins at the poles exhibit trapezoidal shape in time, with longer periods of stationarity, followed by fast switching of the configuration. From a dynamical systems point of view, this spatio-temporal pattern is considered to be ‘antagonistic’. Such dynamics could be based on a perturbation of heteroclinic orbits joining two saddle points in phase space. We analyse such a scenario using a generalisation of the theoretical framework proposed in [12] and provide an example where the time changes in the concentrations follow an ‘antagonistic’ pattern.

2000 MATHEMATICS SUBJECT CLASSIFICATION: 37N25, 37M99, 92B05.

KEYWORDS AND PHRASES: Biological modeling, Protein dynamics, Dynamical systems, Oscillatory behavior.

1. INTRODUCTION

Modern live-cell imaging technologies have demonstrated that bacterial cells exhibit complex spatio-temporal organization of macromolecules. In particular, many proteins localize dynamically to specific subcellular locations where they perform a specific function or influence a fundamental process. Some proteins also undergo spatial oscillations [7]. These proteins include those of the Min system and the Par system in *Escherichia coli* [2, 3, 4, 5, 10], those involved in cell cycle progression and cell differentiation in *Caulobacter crescentus* [6], and those of the Mgl/Frz regulatory system for cell polarity in *Myxococcus xanthus* [1].

M. xanthus is a soil bacterium which moves by means of two gliding motility systems, one of which is based on type IV pili localized to the leading pole. The motility systems and the Frz chemosensory system are regulated by a molecular oscillator built from the proteins MglA, MglB and (so far not identified) members of the Frz family [9, 13]. When the rod-shaped *M. xanthus* cells reverse their direction of movement, certain regulatory proteins (see details below) switch polarity. Hence, the pili are disassembled from the old leading pole and reappear at the new leading pole, and the bacterium begins to move in the opposite direction.

Between reversals (that occur in a highly irregular pattern but with an average reversal period of 15 min [7]), the proteins MglA and MglB are localized in a fixed pattern with MglA-GTP localized near the leading pole, MglA-GDP in the cytoplasm and MglB near the lagging pole [7]. The duration of a reversal

¹ Department of Mathematics and Informatics, Philipps-Universität Marburg, Hans-Meerwein-Str., 35032, Marburg, Germany, (E-mail: rashkov@mathematik.uni-marburg.de)

² Department of Mathematics and Informatics, Philipps-Universität Marburg, Hans-Meerwein-Str., 35032, Marburg, Germany, (E-mail: schmitt@mathematik.uni-marburg.de)

³ Max Planck Institute for Terrestrial Microbiology, Karl-von-Frisch-Str. 10, 35043, Marburg, Germany, (E-mail: sogaard@mpi-marburg.mpg.de)

⁴ Department of Physics, Philipps-Universität Marburg, Renthof 6, 35032, Marburg, Germany, (E-mail: peter.lenz@physik.uni-marburg.de)

⁵ Department of Mathematics and Informatics, Philipps-Universität Marburg, Hans-Meerwein-Str., 35032, Marburg, Germany, (E-mail: dahlke@mathematik.uni-marburg.de)

is significantly shorter ($\sim 30 - 60$ sec) [8], leading to a trapezoidal shape of the time profile of the polar concentrations of MglA and MglB.

In [12] a general model framework for the description of protein oscillations in a bacterium was introduced and analyzed under specific conditions. Accordingly, in [12] the discussed oscillating models were constructed as limit cycles near a saddle point with positive protein concentrations everywhere in the cell.

These cycles showed regular oscillations and their shapes were rather smooth. Observations of *M. xanthus*, however, show protein concentrations which seem rather constant over long times and switch comparatively fast to the opposite poles [7, 8]. In dynamical systems such behaviour is often typical for an orbit oscillating between two saddle points which are connected by a heteroclinic orbit. Solutions near this heteroclinic orbit never reach these saddles but stagnate near them over long times leading to some rather trapezoidal shape of the time curve as observed for *M. xanthus*.

In [12] a reaction-diffusion system was considered that models the protein dynamics of a bacterial cell. A system of reaction-diffusion equations describes the temporal change in concentrations of the proteins in the cytoplasm, at the left and right poles, denoted respectively by $c_i, \ell_i, r_i > 0$:

$$\frac{1}{d_i} - \frac{\partial}{\partial t} c_i(t, x) = \Delta c_i(t, x) \quad (1)$$

$$\frac{1}{d_i} - \frac{d}{dt} \ell_i(t) = \alpha_i(\ell) c_i(t, 0) - \kappa_i(\ell) \ell_i, \quad i = 1, 2 \quad (2)$$

$$\frac{1}{d_i} - \frac{d}{dt} r_i(t) = \alpha_i(r) c_i(t, 1) - \kappa_i(r) r_i. \quad (3)$$

In Eqs. (1)-(3) $\ell(t) = (\ell_i(t))_{i=1}^2, r(t) = (r_i(t))_{i=1}^2$ are vectors of the concentrations of the proteins at the left and right pole at time t , and $c(t, x) = (c_i(t, x))_{i=1}^2$ is the vector of the concentrations in the cytoplasm. The non-negative functions α_i, κ_i are the on- and off-rates for the binding to the poles. Their arguments are the vectors ℓ and r at the left or right pole, respectively.

For a steady state $(\hat{\ell}, \hat{c}(x), \hat{r})$ of the system (1)-(3), it is shown in [12] that the concentration in the cytoplasm is also constant in x , i.e., $\hat{c}_i(x) \equiv \hat{c}_i$. Therefore, we obtain the following relation for the values $(\hat{\ell}_i, \hat{c}_i(x), \hat{r}_i)$,

$$\begin{aligned} \alpha_i(\hat{\ell}) \hat{c}_i &= \kappa_i(\hat{\ell}) \hat{\ell}_i, \\ \alpha_i(\hat{r}) \hat{c}_i &= \kappa_i(\hat{r}) \hat{r}_i, \end{aligned} \quad (4)$$

As long as $\alpha_i > 0$, these imply

$$\hat{c}_i = \frac{\kappa_i(\hat{\ell}) \hat{\ell}_i}{\alpha_i(\hat{\ell})} = \frac{\kappa_i(\hat{r}) \hat{r}_i}{\alpha_i(\hat{r})}. \quad (5)$$

Note, that if $(\hat{\ell}_i, \hat{c}_i(x), \hat{r}_i)$ is a steady state of the system (1)-(3), then so is the mirror point $(\hat{r}_i, \hat{c}_i(x), \hat{\ell}_i)$. For the sake of simplification of the analysis, [12] assumed that the steady state is homogeneous, i.e., $(\hat{\ell}_i, \hat{c}_i(x), \hat{r}_i) := (1, \chi_{[0,1]}, 1)$. That automatically implied that $\alpha_i(\hat{\ell}) = \alpha_i(\hat{r}) = \kappa_i(\hat{\ell}) = \kappa_i(\hat{r})$.

In general, the steady state configuration need not be homogeneous as initially assumed in [12]. Observations in *M. xanthus* suggest concentrations in a steady state at the right and left poles may not be exactly equal, $\hat{\ell} \neq \hat{r}$. Therefore, $\alpha_i(\hat{\ell}) \neq \alpha_i(\hat{r})$, $\kappa_i(\hat{\ell}) \neq \kappa_i(\hat{r})$. If protein concentrations at a pole become very small, the saddle point may be an equilibrium where some protein concentration is zero. This would be a case not covered in [12] as it would be possible that $\alpha_i(\hat{\ell})$ or $\alpha_i(\hat{r}) = 0$ and (5) may not hold anymore.

For assessing the stability properties of such equilibria a generalization of the eigenvalue analysis from [12] is required. The aim now is to analyse the stability properties of the system (1)-(3) under less restricting assumptions (such as unequal diffusion coefficients, non-homogeneous/non-symmetric steady state configuration) in order to obtain different types of periodic orbits, e.g., orbits of trapezoidal shape.

Henceforth, an eigenvalue analysis will be performed for the general system. The notation that will be used is: $D = \text{diag}(d_i)$ is the diffusion matrix, $A = \text{diag}(\alpha_i)$, $K = \text{diag}(\kappa_i)$, $i = 1, \dots, 2$ are matrices of the protein binding and unbinding rates. The system (1)-(3) written in matrix form is then.

$$D^{-1} \frac{\partial}{\partial t} c(t, x) = \nabla^2 c(t, x), \quad (6)$$

$$D^{-1} \frac{d}{dt} \ell(t) = A(\ell) c(t, 0) - K(\ell) \ell, \quad (7)$$

$$D^{-1} \frac{d}{dt} r(t) = A(r) c(t, 1) - K(r) r, \quad (8)$$

Furthermore, we recall the following result about total mass conservation:

Lemma 1 ([12]): Let the coefficients α_i , κ_i , $i = 1, 2$, be continuous functions. Then for any classical solution of the system (6)-(8) with boundary conditions

$$\begin{aligned} \nabla c(0) &= A(\ell) c(t, 0) - K(\ell) \ell, \\ \nabla c(1) &= -A(r) c(t, 1) + K(r) r \end{aligned} \quad (9)$$

the mass

$$m_i(t) := \ell_i(t) + \int_0^1 c_i(t, x) dx + r_i(t), \quad i = 1, 2, \quad (10)$$

is constant, $m_i(t) \equiv m_i(0)$, $i = 1, 2$ for all $t \geq 0$.

The structure of this paper is the following: Section 2 presents a generalized eigenvalue analysis of the system given by Eqs. (6)-(8). Section 3 considers a special asymmetric steady state where the analysis can be simplified, and Section 4 provides a numerical example where periodic orbits of trapezoidal shape occur. Section 5 demonstrates the robustness of this oscillation for a neighbourhood of the parameter space.

2. LINEAR STABILITY ANALYSIS

Eqs. (2) and (3) are linearized for small perturbations \tilde{l} , $\tilde{c}(x)$, \tilde{r} around the steady state $(\hat{\ell}, \hat{c}, \hat{r})$. Then, we obtain a constant-coefficient parabolic system for \tilde{l} , $\tilde{c}(x)$, \tilde{r} ,

$$\begin{aligned} \tilde{c}' &= D\Delta\tilde{c}, \\ \tilde{l}' &= DA(\hat{\ell})\tilde{c}(0) + DV(\hat{\ell})\tilde{l}, \\ \tilde{r}' &= DA(\hat{r})\tilde{c}(1) + DV(\hat{r})\tilde{r}, \end{aligned} \quad (11)$$

where $A(\hat{\ell}) = \text{diag}(\alpha_i(\hat{\ell}))$, $A(\hat{r}) = \text{diag}(\alpha_i(\hat{r}))$. $V(\hat{\ell})$, $V(\hat{r})$ are matrices of partial derivatives evaluated at the poles, whose j -th rows are given by

$$V(\hat{\ell})|_{j\text{row}} = \nabla(c_j \alpha_j - \ell_j \kappa_j)(\hat{\ell}), \quad (12)$$

$$V(\hat{r})|_{j\text{row}} = \nabla(c_j \alpha_j - r_j \kappa_j)(\hat{r}), \quad (13)$$

respectively.

The system (11) has exponential solutions

$$(\tilde{\ell}(t), \tilde{c}(t, x), \tilde{r}(t)) = e^{\lambda t} (\bar{\mathbf{I}}, \bar{\mathbf{c}}(x), \bar{\mathbf{r}}),$$

where the time rate λ determines the stability of the steady state. Then, (11) gives rise to the following eigenvalue problem

$$\begin{aligned} \lambda \bar{\mathbf{c}} &= D \Delta \bar{\mathbf{c}}, \\ \lambda \bar{\mathbf{I}} &= DA(\hat{\ell}) \bar{\mathbf{c}}(0) + DV(\hat{\ell}) \bar{\mathbf{I}}, \\ \lambda \bar{\mathbf{r}} &= DA(\hat{r}) \bar{\mathbf{c}}(1) + DV(\hat{r}) \bar{\mathbf{r}}. \end{aligned} \quad (14)$$

Therefore, if $\det(\lambda D^{-1} - V(\hat{\ell})) \neq 0$ and $\det(\lambda D^{-1} - V(\hat{r})) \neq 0$ these equations can be solved for $\bar{\mathbf{I}}$, $\bar{\mathbf{r}}$,

$$\bar{\mathbf{I}} = (\lambda D^{-1} - V(\hat{\ell}))^{-1} A(\hat{\ell}) \bar{\mathbf{c}}(0), \quad (15)$$

$$\bar{\mathbf{r}} = (\lambda D^{-1} - V(\hat{r}))^{-1} A(\hat{r}) \bar{\mathbf{c}}(1). \quad (16)$$

A substitution into the boundary conditions (9) for \mathbf{c} gives then

$$\nabla \bar{\mathbf{c}}(0) = \lambda D^{-1} \bar{\mathbf{I}} = \lambda D^{-1} (\lambda D^{-1} - V(\hat{\ell}))^{-1} A(\hat{\ell}) \bar{\mathbf{c}}(0), \quad (17)$$

$$\nabla \bar{\mathbf{c}}(1) = -\lambda D^{-1} \bar{\mathbf{r}} = -\lambda D^{-1} (\lambda D^{-1} - V(\hat{r}))^{-1} A(\hat{r}) \bar{\mathbf{c}}(1). \quad (18)$$

Eqns. (14), (17) and (18) define a boundary value eigenproblem for $\bar{\mathbf{c}}$. However, the solutions of the diffusion equation in (14) are exponential functions in space, i.e., $c_i(x) = e^{\mu_i x} a_i + e^{-\mu_i x} b_i$, which may be written in vector form as $\bar{\mathbf{c}} = (c_i(x))_{i=1}^2$

$$\bar{\mathbf{c}}(x) = e^{Mx} \mathbf{a} + e^{-Mx} \mathbf{b}$$

for a diagonal matrix $M := \text{diag}(\mu_i)_{i=1}^2$ such that $\mu_i^2 = \frac{\lambda}{d_i}$ or $M^2 = \lambda D^{-1}$, and $\mathbf{a} := (a_i)_{i=1}^2$, $\mathbf{b} := (b_i)_{i=1}^2 \in \mathbb{C}^2$.

Upon defining the meromorphic functions

$$f(z) := \frac{\sinh \sqrt{z}}{\sqrt{z}}, \quad g(z) := \cosh \sqrt{z},$$

(that yield, e.g., $\cosh(\lambda D^{-1}) = g(\lambda D^{-1}) = \text{diag}(\cosh \sqrt{\frac{\lambda}{d_i}})_{i=1}^2$) we obtain the following lemma for the general case.

Lemma 2: Some $\lambda \neq 0$ is an eigenvalue of the linearized system (14) at the steady state $(\hat{\ell}, \hat{c}, \hat{r})$ if the determinant

$$\begin{vmatrix} A(\hat{\ell})D & V(\hat{\ell})D - \lambda I \\ A(\hat{r})Dg(\lambda D^{-1}) + (\lambda I - V(\hat{r})D)f(\lambda D^{-1}) & \lambda A(\hat{r})f(\lambda D^{-1}) + (\lambda I - V(\hat{r})D)g(\lambda D^{-1}) \end{vmatrix} = 0. \quad (19)$$

Proof: The vectors \mathbf{a} , \mathbf{b} are determined by a substitution into the boundary conditions (17), (18):

$$M(\mathbf{a} - \mathbf{b}) = M^2(M^2 - V(\hat{\ell}))^{-1} A(\hat{\ell})(\mathbf{a} + \mathbf{b}), \quad (20)$$

$$M(e^M \mathbf{a} - e^{-M} \mathbf{b}) = -M^2(M^2 - V(\hat{r}))^{-1} A(\hat{r})(e^M \mathbf{a} + e^{-M} \mathbf{b}), \quad (21)$$

which yields the following system for \mathbf{a} , \mathbf{b} ,

$$A(\hat{\ell})(\mathbf{a} + \mathbf{b}) = (M^2 - V(\hat{\ell}))M^{-1}(\mathbf{a} - \mathbf{b}), \quad (22)$$

$$A(\hat{r})(e^M \mathbf{a} + e^{-M} \mathbf{b}) = -(M^2 - V(\hat{r}))M^{-1}(e^M \mathbf{a} - e^{-M} \mathbf{b}). \quad (23)$$

By setting new variables $\mathbf{u} = \mathbf{a} + \mathbf{b}$, $\mathbf{v} = M^{-1}(\mathbf{a} - \mathbf{b})$, we obtain from (22),

$$A(\hat{\ell})\mathbf{u} - (M^2 - V(\hat{\ell}))\mathbf{v} = 0. \quad (24)$$

We use furthermore the relations

$$e^M \mathbf{a} + e^{-M} \mathbf{b} = (\sinh M)(\mathbf{a} - \mathbf{b}) + (\cosh M)(\mathbf{a} + \mathbf{b}) \quad (25)$$

$$e^M \mathbf{a} - e^{-M} \mathbf{b} = (\sinh M)(\mathbf{a} + \mathbf{b}) + (\cosh M)(\mathbf{a} - \mathbf{b}), \quad (26)$$

where $\sinh M := \text{diag}(\sinh \mu_i)_{i=1}^2$, $\cosh M := \text{diag}(\cosh \mu_i)_{i=1}^2$ are diagonal 2×2 -matrices, to transform (23) to

$$A(\hat{r})(\sinh M)M\mathbf{v} + A(\hat{r})(\cosh M)\mathbf{u} + (M^2 - V(\hat{r}))M^{-1}(\sinh M)\mathbf{u} + (M^2 - V(\hat{r}))M^{-1}(\cosh M)M\mathbf{v} = 0. \quad (27)$$

Since D is a diagonal matrix, M is also diagonal, so M commutes with both $\sinh M$; $\cosh M$. It follows from rearranging the terms in (27) that

$$(A(\hat{r})\cosh M + (M^2 - V(\hat{r}))M^{-1}\sinh M)\mathbf{u} + (A(\hat{r})M\sinh M + (M^2 - V(\hat{r}))\cosh M)\mathbf{v} = 0. \quad (28)$$

The system given by Eqs. (24) and (28) has a nontrivial solution for \mathbf{a} , \mathbf{b} if and only if the determinant

$$\begin{vmatrix} A(\hat{\ell}) & V(\hat{\ell}) - M^2 \\ A(\hat{r})\cosh M + (M^2 - V(\hat{r}))M^{-1}\sinh M & A(\hat{r})M\sinh M + (M^2 - V(\hat{r}))\cosh M \end{vmatrix} = 0. \quad (29)$$

This seems to be an eigenvalue problem for the diagonal matrix M , not the eigenvalue λ itself. However, by a change of basis in Eq. (29) using f , g , we obtain the desired result.

Note: The condition (19) is a transcendental eigenvalue problem for the eigenvalue λ itself. Although it may not be easily analysed in this general form, the determinant of the matrix is evaluated easily and may be used for the numerical computation of eigenvalues.

3. STABILITY ANALYSIS OF AN ASYMMETRIC STEADY STATE

Here we are interested in the stability analysis of a steady state with an asymmetric conformation of protein concentrations. Let us assume for simplicity that the diffusion constants are equal $d_i = d > 0$ for $i = 1, 2$. Without loss of generality we can rescale them to $d = 1$ since this just amounts to rescaling the eigenvalue λ according to the relation $M^2 = \frac{\lambda}{d}I$. Then $M^2 = \lambda I$ and if $\lambda \neq \pm \frac{\pi}{2}i$, we can divide both sides of (28) by $\cosh \lambda$ to obtain an eigenvalue problem for λ only.

Lemma 3: The linearized system at the steady state $(\hat{\ell}, \hat{c}, \hat{r})$ has an eigenvalue $\lambda \neq 0, \pm \frac{\pi}{2}i$ if

$$\begin{vmatrix} A(\hat{\ell}) & V(\hat{\ell}) - \lambda I \\ A(\hat{r}) + (\lambda I - V(\hat{r}))\tau(\lambda) & A(\hat{r})\lambda\tau(\lambda) + (\lambda I - V(\hat{r})) \end{vmatrix} = 0, \quad (30)$$

where $\tau(\lambda) = \frac{\tanh \sqrt{\lambda}}{\sqrt{\lambda}}$.

Note that this problem has an infinite number of solutions, but we are interested only in the solution for λ with the largest real part.

We want to obtain a steady state solution where the total mass $\hat{m}_1 > 0$ of the one protein is concentrated at one pole, while the other protein is not present there. Such a behaviour has been seen experimentally for the proteins MglA and MglB in *M. xanthus*. This amounts to having a steady state distribution (which we index by I) with $\hat{\ell}_I = (\hat{m}_1, 0)$, $\hat{c}_I = (0, \hat{c}_2)$, $\hat{r}_I = (0, \hat{m}_2)$ for $\hat{c}_2, \hat{m}_2 > 0$. Furthermore, the conditions (4) imply

$$\kappa_1(\hat{\ell}_I) = \kappa_1(\hat{m}_1, 0) = 0, \quad (31)$$

$$\alpha_2(\hat{\ell}_I) = \alpha_2(\hat{m}_1, 0) = 0, \quad (32)$$

$$\alpha_2(0, \hat{m}_2) \hat{c}_2 = \kappa_2(0, \hat{m}_2) \hat{m}_2. \quad (33)$$

The first two are satisfied, for example, when $\kappa_1(y_1, y_2) = y_2 \gamma_1(y_1, y_2)$, $\alpha_2(y_1, y_2) = y_2 \beta_2(y_1, y_2)$ for some smooth non-negative functions β_2, γ_1 . Hence, from Eq. (33) it follows that $\beta_2(0, \hat{m}_2) = \frac{\kappa_2(0, \hat{m}_2)}{\hat{c}_2}$, and the partial derivatives satisfy

$$\kappa_{1,1}(y_1, y_2) = y_2 \gamma_{1,1}(y_1, y_2),$$

$$\kappa_{1,2}(y_1, y_2) = \gamma_1(y_1, y_2) + y_2 \gamma_{1,2}(y_1, y_2),$$

and

$$\alpha_{2,1}(y_1, y_2) = y_2 \beta_{2,1}(y_1, y_2),$$

$$\alpha_{2,2}(y_1, y_2) = \beta_2(y_1, y_2) + y_2 \beta_{2,2}(y_1, y_2).$$

In order to apply Lemma 3 we analyse explicitly the matrices $A(\hat{\ell}_I)$, $A(\hat{r}_I)$, $V(\hat{\ell}_I)$, $V(\hat{r}_I)$. Due to Eq. (32), the diagonal matrix

$$A(\hat{\ell}_I) = \begin{pmatrix} \alpha_1 & 0 \\ 0 & 0 \end{pmatrix} \Big|_{(\hat{m}_1, 0)},$$

is singular. In addition to Eqs. (31)-(32), $\alpha_{2,1}(\hat{m}_1, 0) = 0$, $\kappa_{1,1}(\hat{m}_1, 0) = 0$, $\alpha_{2,2}(\hat{m}_1, 0) = \beta_2(\hat{m}_1, 0)$, $\kappa_{1,2}(\hat{m}_1, 0) = \gamma_1(\hat{m}_1, 0)$, which gives

$$V(\hat{\ell}_I) = \begin{pmatrix} 0 & -\hat{m}_1 \gamma_1 \\ 0 & \hat{c}_2 \beta_2 - \kappa_2 \end{pmatrix} \Big|_{(\hat{m}_1, 0)}.$$

On the other hand,

$$A(\hat{r}_I) = \begin{pmatrix} \alpha_1 & 0 \\ 0 & \alpha_2 \end{pmatrix} \Big|_{(0, \hat{m}_2)},$$

and since $\alpha_{2,2}(0, \hat{m}_2) = \beta_2(0, \hat{m}_2) + \hat{m}_2 \beta_{2,2}(0, \hat{m}_2)$ and $\beta_2(0, \hat{m}_2) = \frac{\kappa_2(0, \hat{m}_2)}{\hat{c}_2}$

$$V(\hat{r}_I) = \begin{pmatrix} -\kappa_1 & 0 \\ \hat{c}_2 \alpha_{2,1} - \hat{m}_2 \kappa_{2,1} & \hat{c}_2 \hat{m}_2 \beta_{2,2} - \hat{m}_2 \kappa_{2,2} \end{pmatrix} \Big|_{(0, \hat{m}_2)}.$$

Hence the determinant condition from Eq. (30) for steady state I simplifies to

$$\begin{vmatrix} a'_{11} & 0 & -\lambda & v'_{12} \\ 0 & 0 & 0 & v'_{22} - \lambda \\ a^r_{11} + (\lambda - v^r_{11}) \tau(\lambda) & 0 & a^r_{11} \lambda \tau(\lambda) + \lambda - v^r_{11} & 0 \\ -v^r_{21} \tau(\lambda) & a^r_{22} + (\lambda - v^r_{22}) \tau(\lambda) & -v^r_{21} & a^r_{22} \lambda \tau(\lambda) + \lambda - v^r_{22} \end{vmatrix} = 0,$$

where we have labeled the entries of $A(\hat{\ell}_i)$, $A(\hat{r}_i)$, $V(\hat{\ell}_i)$, $V(\hat{r}_i)$ by a_{ij}^l , a_{ij}^r , v_{ij}^l , v_{ij}^r respectively. A direct computation shows that the determinant factorizes into

$$(\lambda - v_{22}^l)(a_{22}^r + (\lambda - v_{22}^r)\tau(\lambda)) \begin{vmatrix} a_{11}^l & -\lambda \\ a_{11}^r + (\lambda - v_{11}^r)\tau(\lambda) & a_{11}^r \lambda \tau(\lambda) + \lambda - v_{11}^r \end{vmatrix} = 0. \quad (34)$$

Next we analyse the matrix (30) for the mirror conuguration II , where $\hat{\ell}_{II} = (0, \hat{m}_2)$, $\hat{c}_{II} = (0, \hat{c}_2)$, $\hat{r}_{II} = (\hat{m}_1, 0)$. It is easy to see that due to symmetry $A(\hat{\ell}_{II}) = A(\hat{r}_I)$, $A(\hat{r}_{II}) = A(\hat{\ell}_I)$, $V(\hat{\ell}_{II}) = V(\hat{r}_I)$, $V(\hat{r}_{II}) = V(\hat{\ell}_I)$. Furthermore, again because of symmetry, it is clear that the stability properties of the steady state II are the same as those of the steady state I .

Both steady states I and II have the same eigenvalues that are solutions of the equations

$$0 = \lambda - v_{22}^l, \quad (35)$$

$$0 = a_{22}^r + (\lambda - v_{22}^r)\tau(\lambda), \quad (36)$$

$$0 = \lambda^2 \tau(\lambda) + (a_{11}^l a_{11}^r - v_{11}^l) \lambda \tau(\lambda) + (a_{11}^l + a_{11}^r) \lambda - a_{11}^l v_{11}^r, \quad (37)$$

which can be solved numerically for λ .

4. NUMERICAL EXAMPLE

Here we provide a particular example of a system where oscillations are based on perturbed heteroclinic orbits. As in [12], we place some restrictions on the interaction terms α_i , κ_i in order to simplify the analysis of the matrix problem. We assume that $\kappa_{1,1} = \kappa_{2,1} \equiv 0$ (in other words, the first protein does not actively repel any protein from the poles).

We study the dynamical system (1)-(3) where the interaction functions and diffusion coefficients are given by

$$\begin{aligned} d_1 &= d_2 = 1, \\ \alpha_1(y_1, y_2) &= 1 - p + p y_1^2, \\ \alpha_2(y_1, y_2) &= (0.8 + 0.2 y_1) y_2, \\ \kappa_1(y_1, y_2) &= \frac{2 y_2}{1 + y_2}, \\ \kappa_2(y_1, y_2) &= \frac{4}{3 + y_2}. \end{aligned} \quad (38)$$

Furthermore, the total mass of each protein equals 3 mass units.

With this choice of interaction functions, the following points are steady states of the system (1)-(3):

- I (homogeneous), $(\hat{\ell}_i, \hat{c}_i(x), \hat{r}_i) := (1, 1, 1)$, $i = 1, 2$.
- II , $\hat{\ell} = (3, 0)$, $\hat{r} = (0, 2)$, $\hat{c} = (0, 1)$ because

$$\ell'_1 = \alpha_1(3, 0) \cdot 0 - \underbrace{\kappa_1(3, 0) \cdot 3}_{=0} = 0,$$

$$\ell'_2 = \alpha_2(3, 0) \cdot 1 - \underbrace{\kappa_2(3, 0) \cdot 0}_{=0} = 0,$$

$$r'_1 = \alpha_1(0, 2) \cdot 0 - \kappa_1(0, 2) \cdot 0 = 0,$$

$$r'_2 = \underbrace{\alpha_2(0, 2) \cdot 1}_{=1.6} - \underbrace{\kappa_2(0, 2) \cdot 2}_{=1.6} = 0.$$

The ‘mirror’ steady state II’, $(\hat{\ell}, \hat{c}, \hat{r})$ for $\hat{\ell} = (0, 2)$, $\hat{r} = (3, 0)$, $\hat{c} = (0, 1)$ possesses the same stability properties as shown in the previous Section.

Note that the homogeneous steady state I, $(\hat{\ell}_i, \hat{c}_i(x), \hat{r}_i) := (1, 1, 1)$, $i = 1, 2$ is unstable. For $p = 0.95$, there are two eigenvalues with positive real part $\lambda_1 = 0.33619$, $\lambda_2 = 0.43814$. In fact, for $p > 0.9412$, there are 2 positive eigenvalues for the homogeneous steady state.

We compute the eigenvalues with positive real part at the steady state II using the formula (35)-(37), which have the form

$$0 = \lambda - \frac{1}{15}, \quad (39)$$

$$0 = \frac{8}{5} + \left(\lambda - \frac{8}{25} \right) \tau(\lambda), \quad (40)$$

$$0 = \lambda^2 \tau(\lambda) + \frac{257}{150} \lambda \tau(\lambda) + \frac{153}{20} \lambda + \frac{152}{15}. \quad (41)$$

A numerical computation shows that only the first equation has a solution with $\text{Re } \lambda > 0$, and that is $\lambda = \frac{1}{15}$. The other two equations do not allow such solutions. In a neighbourhood of 0, both

$$f_1(z) = \frac{8}{5} + \left(z - \frac{8}{25} \right) \tau(z), \quad (42)$$

$$f_2(z) = z^2 \tau(z) + \frac{257}{150} z \tau(z) + \frac{153}{20} z + \frac{152}{15}, \quad (43)$$

are holomorphic functions. Both f_1, f_2 map the right half-plane $\text{Re } z > 0$ to the right side of the curves shown in Fig. 1.

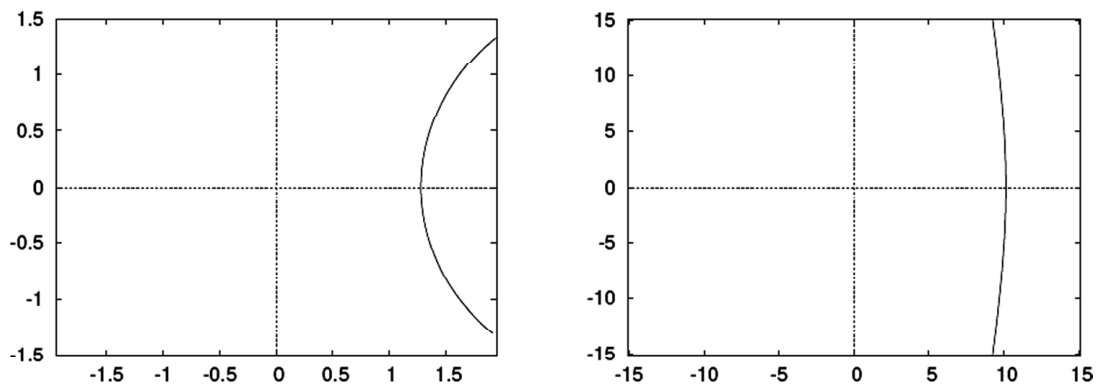


Figure 1: Image of the Right Half-Plane Under f_1 (Left), f_2 (Right)

Figure 2 shows the temporal evolution of ℓ_1, ℓ_2 for $p = 0.95$. The solution of Eqs. (1)-(3) oscillates between the two saddle points II and II’ and remains in the vicinity of both over a longer time.

Note that if $p = 1$, there is a pair of additional steady states appearing between I, II and II’,

- * III, given by $\hat{\ell}_{\text{III}} = (0, 0)$, $\hat{r}_{\text{III}} = (2.4131886, 2.4251653)$, $\hat{c}_{\text{III}} = (0.5868114, 0.5748347)$ and its ‘mirror’ image III’; III is strongly attracting, which prevents periodic solutions of the dynamical system.
- * IV, given by $\hat{\ell}_{\text{IV}} = (0, 0)$, $\hat{r}_{\text{IV}} = (0.5590642, 2.1478209)$, $\hat{c}_{\text{IV}} = (2.4409358, 0.8521791)$ together with its ‘mirror’ image IV’. IV has a single eigenvalue with positive real part, 0.9444449.

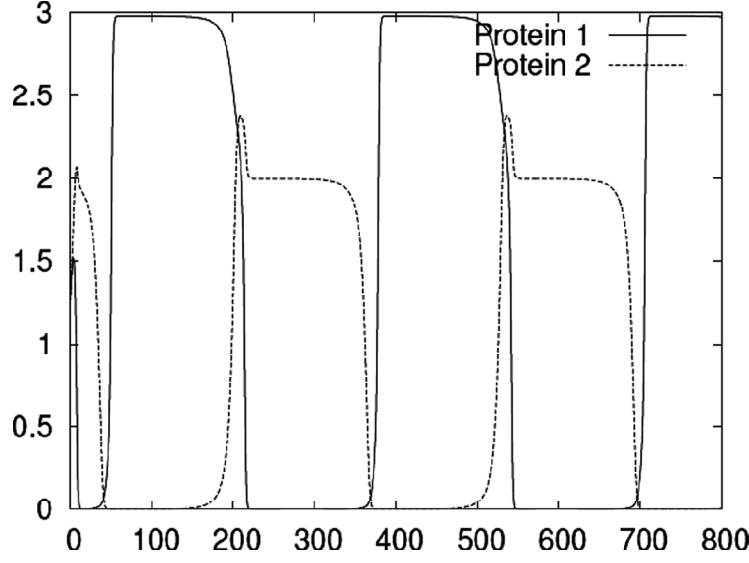


Figure 2: Proteins Display “Antagonistic” Pattern at the Left Pole

The steady state configurations III and IV are obtained by solving numerically the equilibrium equations. These configurations, however, do not correspond to the dynamics that we are interested in.

5. PARAMETER SCAN

It is always essential to study the robustness of the proposed model against parameter variation. We parameterize Eq. (38) taking into account the equilibrium conditions. The interaction functions have the form

$$\begin{aligned}
 d_1 &= d_2 = 1, \\
 \alpha_1(y_1, y_2) &= 1 - a_1 + a_1 y_1^2, \\
 \alpha_2(y_1, y_2) &= \left(\frac{a_2 + 1}{a_2 + 2} + \frac{y_1}{a_2 + 2} \right) y_2, \\
 \kappa_1(y_1, y_2) &= \frac{(1 + a_3) y_2}{a_3 + y_2}, \\
 \kappa_2(y_1, y_2) &= \frac{1 + a_2}{a_2 + y_2}.
 \end{aligned} \tag{44}$$

For $a_2 = 3$, $a_3 = 1$ we obtain the particular example (38) from Section 4.

As in [12] we perform a parameter scan to find the range where the system (1)-(3) with (44) has oscillatory solutions. We search for the range $(a_i)_{i=1}^3$ where both the homogeneous steady state I and the asymmetric steady state II are unstable.

The numerical simulations are performed on a discrete grid with $n = 100$ points. The initial value problem is solved in a time interval $[0, 1000)$. In doing so, we, for simplicity, again focus on the special case $d_1 = d_2 = 1$. We systematically vary the set of parameters $(a_i)_{i=1}^3$ describing the reaction rates in (44) in order to determine the range where stable oscillatory solutions occur. The corresponding range of parameters $(a_i)_{i=1}^3$ within the cube $[0, 4]^3$ is shown in Fig. 3. In fact, oscillations occur also for $a_3 > 4$, so that the set is not bounded in the a_3 -direction.

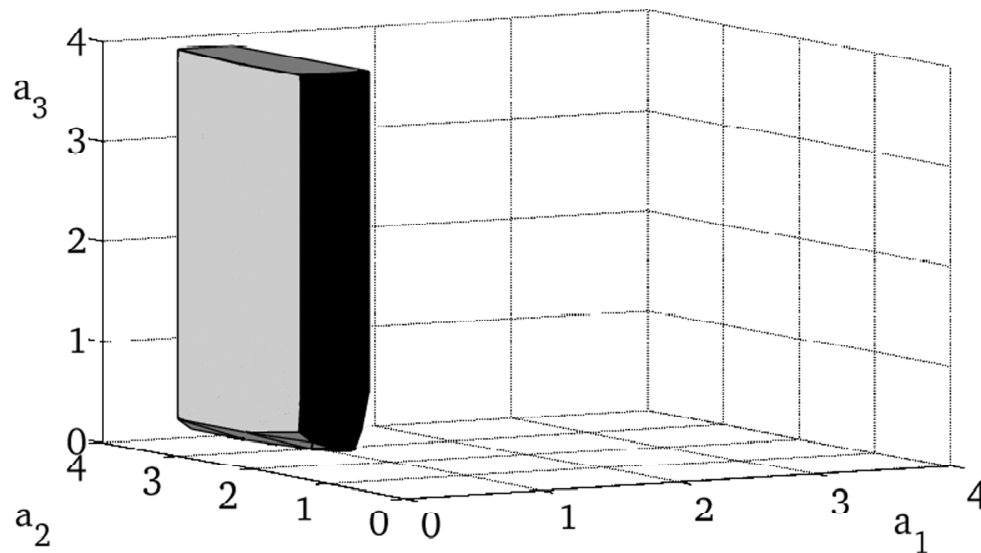


Figure 3: Parameter Range (a_1, a_2, a_3) in which the System Exhibits Stable Oscillatory Solutions

6. CONCLUSION

We have proposed a generalization of the mathematical model derived in [12]. As an application of this framework, we have found a set of interaction functions that produces oscillations consisting of longer periods of stationary protein concentrations near the poles that are followed by fast diffusion to the opposite poles. This self-sustaining oscillator relies on the existence of a pair of saddle points joined by a heteroclinic orbit to produce nearly perfect ‘antagonistic behavior’. Numerical investigations demonstrate the robustness of the model by establishing a large parameter range where oscillations occur. The dynamical system produces behaviour which is similar to the experimentally observed oscillatory protein dynamics in *M. xanthus*. However, one main difference remains: the dynamics of MglA and MglB is highly irregular. In future work, we will investigate if such a behavior can be simply explained by molecular noise or requires more elaborate mechanisms such as, e.g., an external trigger.

ACKNOWLEDGEMENT

This work has been supported by the Center for Synthetic Microbiology (SYNMIKRO) in Marburg, promoted by the LOEWE Excellence Program of the state of Hessen, Germany.

REFERENCES

- [1] Bulyha I., Hot E., Huntley S., and Sogaard-Andersen L., (2011), GTPases in Bacterial Cell Polarity and Signaling, *Cur. Opin. Microbiol.*, **14**, 726-733.
- [2] Gerdes K., Howard M., and Szardenings F., (2010), Pushing and Pulling in Prokaryotic DNA Segregation, *Cell*, **141**, 927-942.
- [3] Howard M., Rutenberg A. D., and de Vet S., (2001), Dynamic Compartmentalization of Bacteria: Accurate Division in *E. Coli*, *Phys. Rev. Let.*, (87) 21, 278102.
- [4] Huang K. C., Meir Y., and Wingreen N. S., (2003), Dynamic Structures in Escherichia Coli: Spontaneous Formation of MinE Rings and MinD Polar Zones, *PNAS*, (100) 22, 12724-12728.
- [5] Kruse K., (2002), A Dynamic Model for Determining the Middle of Escherichia Coli, *Biophys. J.*, **82**, 618-627.
- [6] Laub M. T., Shapiro L., and McAdams H. H., (2007), Systems Biology of Caulobacter, *Ann. Rev. Genet.*, **41**, 429-441.
- [7] Lenz P., and Sogaard-Andersen L., (2011), Temporal and Spatial Oscillations in Bacteria, *Nat. Rev. Micro.*, **9**, 565-577.
- [8] Leonardy S., Bulyha I., and Sogaard-Andersen L., (2008), Reversing Cells and Oscillating Proteins, *Mol. BioSystems*, **4**, 1009-1014.
- [9] Leonardy S., Miertzschke M., Bulyha I., Sperling E., Wittinghofer A., and Sogaard-Andersen L., (2010), Regulation of Dynamic Polarity Switching in Bacteria by a Ras-Like G-Protein and Its Cognate GAP, *EMBO J.*, **29**, 2276-2289.

-
- [10] Lutkenhaus J., (2007), Assembly Dynamics of the Bacterial MinCDE System and Spatial Regulation of the Z ring, *Ann. Rev. Biochem.*, **76**, 539-562.
- [11] Miertzschke M., Koerner C., Vetter I. R., Keilberg D., Hot E., Leonardy S., Bulyha I., Søgaard-Andersen L., and Wittinghofer A., (2010), Regulation of Dynamic Polarity Switching in Bacteria by a Ras-Like G-Protein and Its Cognate, *EMBO J.*, **30**, 4185-4197.
- [12] Rashkov P., Schmitt B. A., Søgaard-Andersen L., Lenz P., and Dahlke S., (2012), A Model of Oscillatory Protein Dynamics in Bacteria, *Bull. Math. Bio.*, **74**(9), 2183-2203.
- [13] Zhang Y., Franco M., Ducret A., and Mignot T., (2010), A Bacterial Ras-Like Small GTP-Binding Protein and Its Cognate GAP Establish a Dynamic Spatial Polarity Axis to Control Directed Motility, *PLoS Biol.*, **8**: e1000430.